

Analytical Design of Compact Multiband Bandpass Filters with Multiconductor Transmission Lines and Shunt Open Stubs

Mario Pérez-Escribano , Enrique Márquez-Segura *  and Juan José Sánchez-Martínez 

Telecommunication Research Institute (TELMA), E.T.S. Ingeniería de Telecomunicación, Universidad de Málaga, Bulevar Louis Pasteur 35, 29010 Málaga, Spain

* Correspondence: ems@ic.uma.es

Abstract: A compact topology for implementing compact multiband bandpass filters is presented in this paper. To achieve the desired frequency response, two identical short-circuited multiconductor transmission lines (MTLs) and properly connected shunt open stubs are interconnected. Using this configuration, it is possible to design multiband bandpass filters effortlessly. As both the MTLs and the stubs are distributed elements, spur-line band-stop filters are added to mitigate the first replica of the structure's frequency response. To assess the behavior of the developed filter design procedure, a prototype consisting of a six fingers-MTL and two shunt open stubs has been designed, manufactured, and analyzed, showing excellent agreement between analytical and measured results, considering that no simulation or optimization process has been performed during the design process, just for result verification. Furthermore, it is possible to establish a design criterion that allows the fast and reliable synthesis of multiband responses by varying just a small number of geometrical parameters of the MTLs and the corresponding stubs.

Keywords: filter design; multiband bandpass filter; multiconductor transmission lines



Citation: Pérez-Escribano, M.; Márquez-Segura, E.; Sánchez-Martínez, J.J. Analytical Design of Compact Multiband Bandpass Filters with Multiconductor Transmission Lines and Shunt Open Stubs. *Electronics* **2023**, *12*, 1945. <https://doi.org/10.3390/electronics12081945>

Academic Editor: Dimitra I. Kaklamani

Received: 24 March 2023

Revised: 17 April 2023

Accepted: 19 April 2023

Published: 20 April 2023



Copyright: © 2023 by the authors. Licensee MDPI, Basel, Switzerland. This article is an open access article distributed under the terms and conditions of the Creative Commons Attribution (CC BY) license (<https://creativecommons.org/licenses/by/4.0/>).

1. Introduction

Nowadays, multi-band services and applications such as IoT (Internet of Things), or wireless local area networks demand using several frequency bands simultaneously and using compact devices. The main reason is that the use of several bands simultaneously improves communication performance, increases network capacity, and reduces interference. In addition, the devices should be as compact as possible with higher performance so that they can be used in small sensors or small gadgets. For that reason, researchers are focused on how to achieve multi-band elements, especially for communication systems, such as antennas [1], amplifiers [2], or filters [3]. Concretely and related to this work, many RF and microwave applications need compact filters with low losses and multi-band operation without increasing the area dedicated to frequency selective devices. Traditionally, microstrip filters have been used in different topologies, like step-impedance resonators [4], interdigital capacitors [5], or a combination of both [6]. In recent years, several alternatives have arisen in the literature, proposing different technologies to create multi-band responses, including filters based on Acoustic-Wave-Lumped-Element-Resonators [7] or split-type filters [8].

Coupled lines have been used traditionally in many applications to develop filters with appropriate frequency responses. One of their most important advantages is that, typically, an analytical model allows designers to control the main parameters of the filters. When increasing the number of fingers in MTLs, a great variety of responses can be obtained because a greater range of impedance and coupling factor values can be achieved. This is only possible as the coupled lines are alternately interconnected with wire bondings to eliminate undesired TEM (transverse electromagnetic) modes inherent to multiconductor structures. In this sense, MTLs have been successfully used for synthesizing wide and ultra-wideband differential [9] or dual-band bandpass filters [10]. Specifically, in

ref. [10], a procedure for the synthesis of Chebyshev-type filters designed from a dual-band transformation was proposed [11], where both bands have the same bandwidth.

The use of MTLs for synthesizing filters with three passbands is discussed in this paper. A novel prototype, composed of two spur-line filters, two identical short-circuited MTLs, and several shunt open stubs, is presented and assessed through experimental validation. It is noteworthy that, with this configuration, filter parameters can be controlled by varying the even and odd mode impedances and the electrical lengths of the MTLs and the stubs. This structure, compared with [10], introduces the independence of the selected bands. Furthermore, it presents a very straightforward design procedure if examined with other previous works [12], taking advantage of the intrinsic multiconductor frequency response. Additionally, to improve out-of-band frequency response, wire-bondings have been added in the middle of the MTLs, whereas two spur-line filters are used to mitigate the first replica of the filter frequency response.

2. Circuit Analysis

The proposed topology is shown in Figure 1. It is composed of two identical short-circuited MTLs, several shunt open stubs (by simplicity, only two are depicted in Figure 1), and spur-line sections at the input and output of the filter. The analysis is based on the one in [10]. In short, the S-parameters from the transmission line equivalent model are computed and considered to obtain a proper filtering function, and finally, the circuit design parameters. The exact analysis of the short-circuited multiconductor transmission lines was thoroughly carried out in [13].

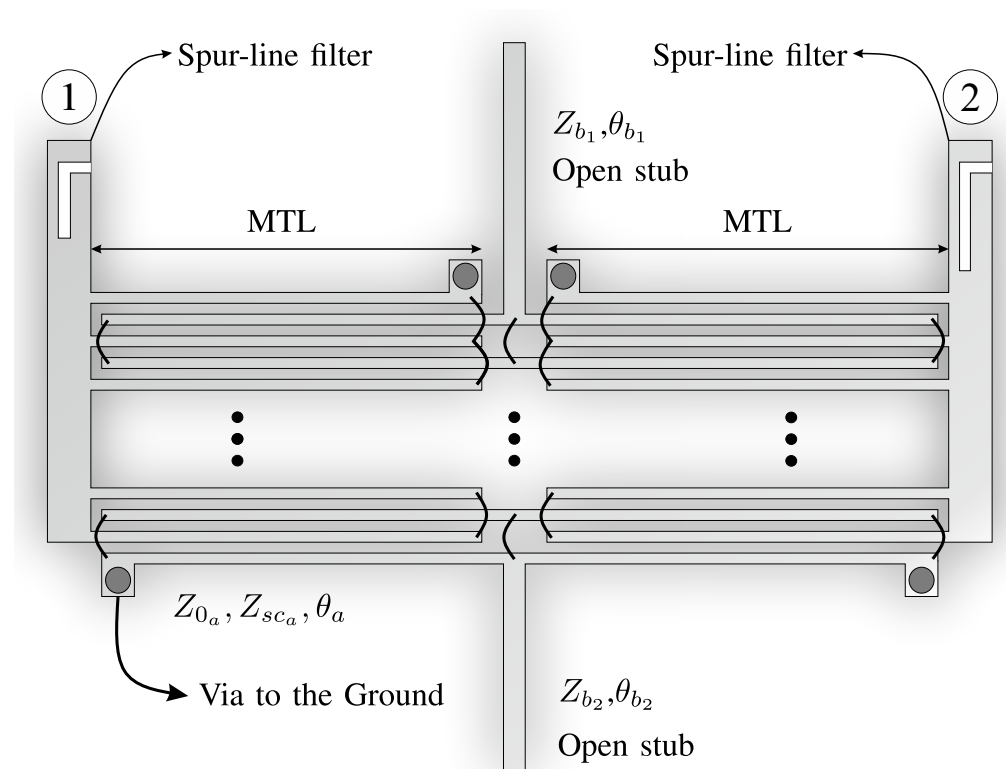


Figure 1. Layout of the proposed circuit for the analyzed multiband bandpass filter.

On the one hand, the transmission-line equivalent model consists of a transmission-line section and two shunt short-circuited stubs with characteristic impedances Z_{0a} and Z_{sc_a} , respectively. The values of these impedances are given by [14]

$$Z_{0a} = \frac{2}{(k - 1)(Y_{00} - Y_{0e})} = \frac{2Z_{0e}Z_{0o}}{(k - 1)(Z_{0e} - Z_{0o})}, \tag{1}$$

$$Z_{sc_a} = Z_{0e} \left(1 + \frac{(k - 2)Z_{0o}}{Z_{0e} + Z_{0o}} \right)^{-1}, \tag{2}$$

where Z_{0e} and Z_{0o} are the even- and odd-mode impedances of a pair of coupled lines, and k is the number of conductors. θ_a is the electrical length of a MTL, computed as the arithmetic mean value of the even- and odd-mode electrical lengths.

On the other hand, the open stubs are defined by their characteristic impedance (Z_{b_i}) and electrical length (θ_{b_i}), whereas the equivalent model of the spur-line filters is composed by a transmission line section and a shunt open stub. Their characteristic impedances, Z_{sl1_j} and Z_{sl2_j} , can be calculated from ref. [15]

$$Z_{sl1_j} = \frac{Z_{0o_{sl_j}} + Z_{0e_{sl_j}}}{2} \tag{3}$$

$$Z_{sl2_j} = \frac{Z_{0e_{sl_j}} \left(\frac{Z_{0e_{sl_j}} + Z_{0o_{sl_j}}}{2} \right)}{Z_{0o_{sl_j}}}, \tag{4}$$

where $Z_{0e_{sl_j}}$ and $Z_{0o_{sl_j}}$ are the even- and odd-mode impedances of the pair of coupled lines that forms the filter, and the electrical length, θ_{sl_j} , is calculated again as the arithmetic mean value of the even- and odd-mode electrical lengths [16].

The complete circuit model is presented in Figure 2. The total S-parameter matrix can be obtained by cascading the transmission parameters of every section in the equivalent model.

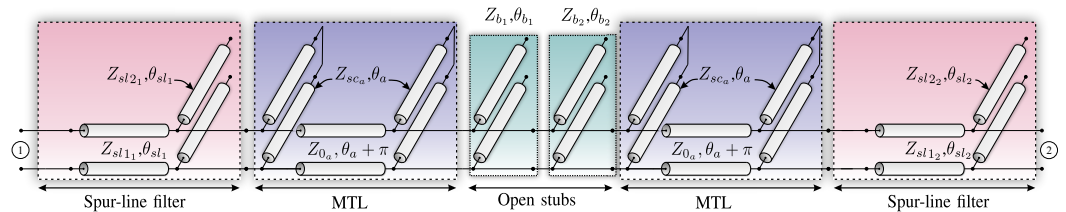


Figure 2. Equivalent circuit model for the proposed filter.

3. Design Considerations

The operation of the proposed filter is based on splitting the wide frequency band of the MTLs by forcing transmission zeros inside it, using the appropriate shunt stubs, as shown in Figure 1. These real transmission zeros will be used to get a good rejection for out-of-band signals and to improve the isolation between adjacent bands.

3.1. Multiconductor Transmission Lines

MTL design is the first step that must be taken. One of the most important advantages of using MTLs instead of a pair of coupled lines is the feasibility of synthesizing a wide range of different impedance values compared with a pair of coupled lines. This fact can be used to increase the slope of filter skirts. The achievable values of Z_{0a} and Z_{sc_a} as a function of line width W and spacing S for a different number of conductors are represented in [9] (Figure 3). That plot was calculated using the Rogers 4350B substrate, with a dielectric constant of 3.66, a loss tangent of 0.0031, and a thickness of 30 m. The same substrate is used in the analyzed and manufactured prototypes in this work. As can be seen, by increasing the number of conductors or reducing the space between them, it is possible to

achieve lower values of Z_{0a} , which, therefore, increases the design possibilities concerning the use of traditional pairs of coupled lines.

Transmission zeros inherent to the MTL are located at $\theta_a = n\pi$, $n = 0, 1, 2, 3, \dots$. However, the exact position of the zeros will vary with the MTL parameters. For instance, bandwidth will be wider and more selective when decreasing both finger width and gap spacing between them, which is equivalent to increasing the coupling factor. The analytical bandwidth of a 6-finger MTL 10 mm long is depicted in Figure 3 for several finger widths and separations. As seen, bandwidth will be wider when decreasing both parameters. Another aspect that must be taken into consideration is MTL finger interconnection. When connecting them, their real length is greater than the one calculated without considering the interconnection. This fact provokes a resonance close to the transmission zero when the length is equal to $\lambda/2$. Nevertheless, this can be effortlessly corrected by adding wire bondings connecting alternate lines in the middle of the MTL. Doing it guarantees that the alternate lines maintain the same voltage in the middle of the MTL. Therefore, the propagation of undesired TEM modes is avoided, so resonances are eliminated. Higher-frequency resonances and replicas will be mitigated by the spur-line sections at input and output ports.

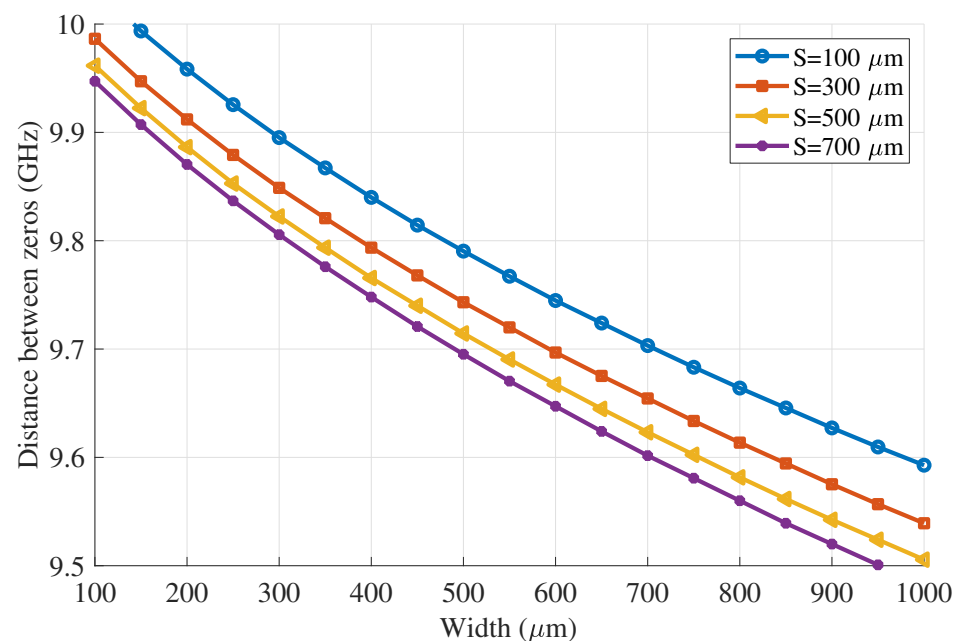


Figure 3. Analytical values of MTL bandwidth for different finger widths (W) and separations (S).

3.2. Open Stubs

On the one hand, the role of the open stubs included in the design is to force real transmission zeros in the middle of the MTL's passband. For this reason, the stubs will work as quarter-wave transformers, imposing short-circuit conditions on the structure at the desired frequency. When doing it, transmission zeros inherent to the stubs are located at $\theta_{b_i} = n\frac{\pi}{2}$, $n = 1, 3, 5, \dots$. Theoretically, N transmission zeros can be forced by N open stubs inside the MTL band, and consequently, there will be $N + 1$ bands. In real cases, transmission media and geometry limit the number of possible stubs. The tee junction and open-ended effect in the shunt stubs [17] must be considered carefully to improve the design precision. To increase the order of the filter, it would be enough to choose stubs with greater bandwidth, such as radial stubs. On the other hand, spur lines are used to mitigate the undesired high-frequency replicas of the MTLs and the stubs, and they will be located at the input and the output of the filter.

3.3. Design Criteria

To design the proposed filter, the first step is to choose the MTL bandwidth through its length and position the zeros with the stubs, where its electrical length is equal to $\lambda/4$. To achieve a more selective filter and increase the bandwidth, it is only necessary to increase the coupling of the MTL or decrease the impedance of the stub, making it possible to obtain very selective responses without the need to optimize or perform electromagnetic simulations, just using the analytical model. The process is summarized as follows:

1. Choose MTL bandwidth positioning its first transmission zero (3) ($\theta_a = \pi$).

$$l_{MTL} = \frac{c_0}{2f_{zero3}\sqrt{\epsilon_{eff_{MTL}}}}, \quad (5)$$

where

$$\sqrt{\epsilon_{eff_{MTL}}} = \frac{\sqrt{\epsilon_{eff_e}} + \sqrt{\epsilon_{eff_o}}}{2}. \quad (6)$$

2. Position the inner band zeros (1, 2) with the stubs ($\theta_{b_i} = \frac{\pi}{2}$).

$$l_{stub} = \frac{c_0}{4f_{zero1,2}\sqrt{\epsilon_{eff_{stub}}}}. \quad (7)$$

3. Select the MTL and stubs impedances using the design criteria for the first prototype of [10].
4. Choose the spur-line section parameters to mitigate the first replica of the structure ($\theta_{sl_i} = \frac{\pi}{2}$).

$$l_{spur} = \frac{c_0}{6f_{zero_{MTL}}\sqrt{\epsilon_{eff_{spur}}}}. \quad (8)$$

Step Three is especially relevant. As can be seen, the slopes of the pass-bands can be improved by increasing the number of fingers on the multiconductor transmission line and reducing the distance between them. This is equivalent to increasing the coupling and reducing the MTL impedance. By increasing the width of the stub (reducing its impedance), it is also possible to get higher slopes. The central frequency of each band is calculated from the inner band zeros (1, 2), provoked by stubs.

4. Results

As a design example, a prototype fabricated using Rogers 4350B substrate ($h = 30$ m) has been manufactured. The physical dimensions of the filter are summarized in Table 1. It is noteworthy that a problem in manufacturing tolerances caused a variation in the impedances of the original circuit design. Two identical short-circuited MTLs and two open stubs of different lengths and the same widths are interconnected, as depicted in Figure 4. When considering the dispersion model for microstrip and coupled lines, the values of the characteristic impedances are $Z_{0_a} = 56.5 \Omega$ (69.3 Ω in the manufactured prototype), $Z_{sc_a} = 91.9 \Omega$ (99.1 Ω) and $Z_{0_b} = 140.6 \Omega$ (158.6 Ω) respectively, using a reference impedance $Z_0 = 50 \Omega$. Figure 5 shows the difference between the simulated S-parameters of the designed and manufactured filters, as well as a photograph of the simulated filter. Simulations have been performed using the full-wave electromagnetic simulator ANSYS HFSS. As seen, the main difference is a small displacement of the bands and mismatch, but despite the huge manufacturing tolerance, this structure is very robust and reliable, and results hardly vary.

The first transmission zero of the MTL must be located at 9.55 GHz, whereas the zeros provoked by the open stubs should be located at 3.91 GHz and 5.87 GHz, respectively. It could be used for WiFi and other applications, such as IoT or vehicle-to-vehicle communications where high slopes are not critical and compact structures are needed. The theoretical S-parameters of the MTLs are calculated using the model proposed in [14]. Once these parameters have been calculated, ABCD two-port parameters for both the MTL and stub

are computed. No electromagnetic simulation or optimization has been carried out for this design. Analytical, simulated, and measured results are shown in Figure 6. As seen, there is an excellent agreement between analytical and measured results, which are even more similar than simulated results. The small difference in bandwidth and matching is due to fabrication tolerances, which denote the robustness of the technology presented, even when manufacturing errors are made. Finally, a comparison with others based on coupled line filters found in the state-of-the-art is summarized in Table 2. In this table, RL denotes the minimum return losses, IL the maximum insertion losses, λ_g is the guided wavelength at the center frequency (f_0) of the lower passband, and FBW is the fractional bandwidth of that band. Furthermore, it includes the substrate used in each case. As can be seen, the proposed filter improves on the performance of those published, being more compact and extremely easy to design. Around 8.6 GHz, a resonance can be observed, caused by the length of the wire bondings. As the number of fingers increases, the length of the bonding increases, and resonance appears as predicted in [18]. Special attention must be taken when making the wire bondings, keeping them as short as possible. Figure 6 shows a simulation with higher values than the real value in the prototype to show how reducing this length controls the amplitude of resonance.

Table 1. Physical dimensions of the simulated filters.

Parameter	Design Value	Manufactured
MTL number of fingers	6	6
MTL finger width	170 μm	123 μm
MTL finger separation	200 μm	238 μm
MTL finger length	9.5 mm	9.46 mm
Stub #1 width	130 μm	83 μm
Stub #1 length	8 mm	7.97 mm
Stub #2 width	130 μm	83 μm
Stub #2 length	12 mm	11.96 mm
Spur-line width	150 μm	192 μm
Spur-line gap	150 μm	195 μm
Spur-line length	3.25 mm	3.21 mm

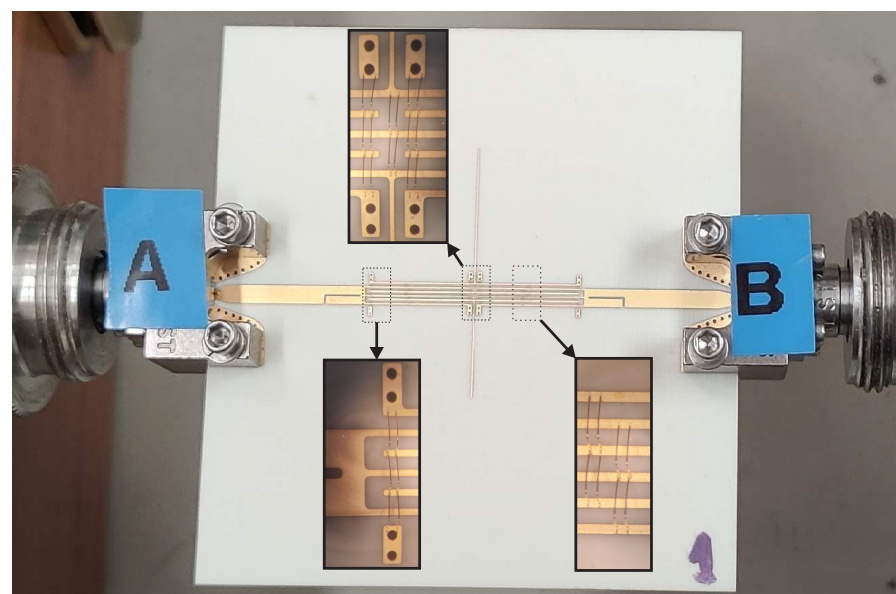


Figure 4. Photograph of the manufactured prototype with 6-finger short-circuited MTLs and two shunt open stubs. Detail of the wire-bondings used to guarantee equal potential at the ends and in the middle of the structure are detailed in sub-pictures.

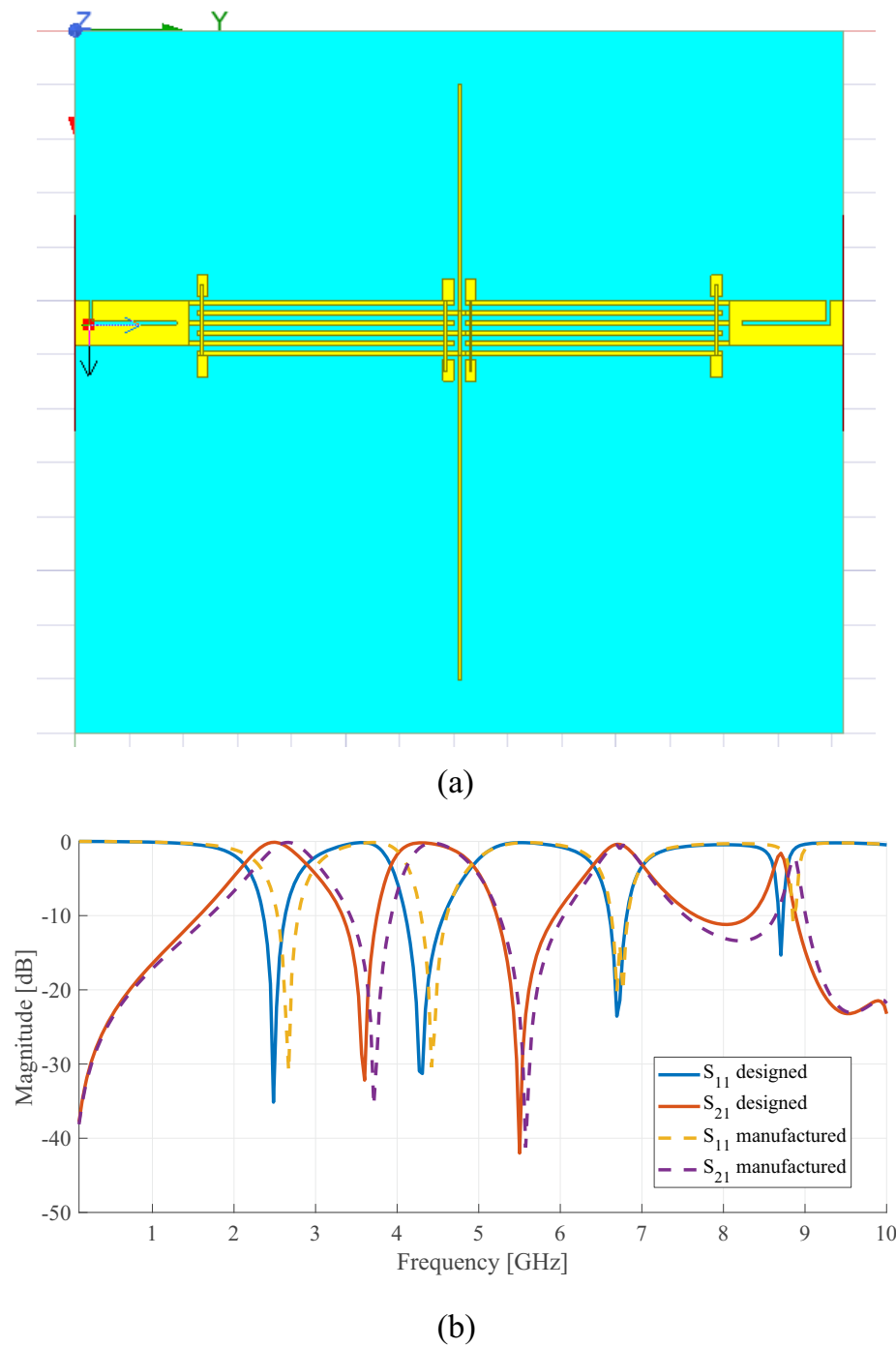


Figure 5. (a) Photograph of the simulated filter (b) simulated scattering matrix elements (S_{11} and S_{21}) of the designed and manufactured prototype.

Table 2. Comparison among the proposed multiband filters and published ones.

Filter	RL (dB)	IL (dB)	Size ($\lambda_g \times \lambda_g$)	f_0 (GHz)	FBW (%)	Substrate
[3]	16.7	4.6	0.66×0.42	1.54	11	$\epsilon = 2.55$
[6]	17.12	2.88	0.35×0.25	1.8	5.5	GML 1000
[19]	8.2	1.8	1.29×1.33	0.415	55.4	Rogers RO4003C
[20]	17.9	2.69	0.81×0.58	3.3	3.57	Rogers RO4003C
[21]	20	4.25	0.46×0.22	1	0.08	Rogers RO4003C
Proposed Filter	16.5	1.3	0.29×0.29	2.5	40	Rogers RO4350B

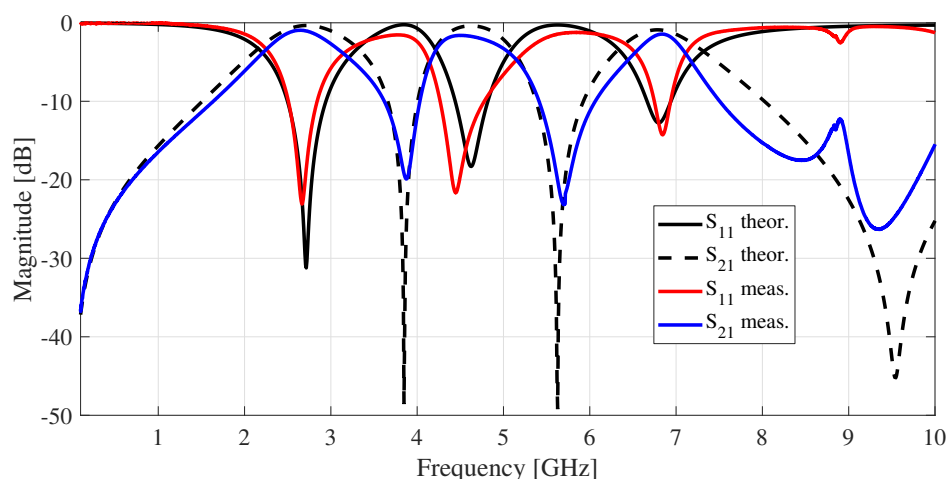


Figure 6. Analytical, electromagnetic simulated using HFSS and measured scattering matrix elements (S_{11} and S_{21}) of the proposed prototype.

5. Conclusions

The analytical design of a novel topology for multiband bandpass filters using multiconductor transmission lines has been addressed in this letter. For this purpose, two identical short-circuited MTLs interconnected with several shunt open stubs have been proposed. Using this topology, a multiband bandpass response is obtained as the open stubs create real transmission zeros in the MTL passband. Changing MTL and stubs parameters makes it possible to select each band's central frequencies and bandwidths effortlessly. Three different passbands have been considered in this work. To assess the developed theory, results from one prototype are considered, showing excellent agreement between the theoretical model and measurements, even when considering manufacturing errors. It is noteworthy that there were no optimization processes or electromagnetic simulations throughout the design procedure provided in this contribution. Spur-line sections have been added to the circuit to mitigate the effect of the frequency response replicas inherent to distributed structures.

Author Contributions: Conceptualization, M.P.-E. and E.M.-S.; methodology, M.P.-E. and E.M.-S.; software, M.P.-E.; validation, M.P.-E., E.M.-S. and J.J.S.-M.; formal analysis, M.P.-E. and E.M.-S.; investigation, M.P.-E., E.M.-S. and J.J.S.-M.; resources, M.P.-E.; writing—original draft preparation, M.P.-E.; writing—review and editing, E.M.-S.; visualization, E.M.-S.; supervision, E.M.-S. and J.J.S.-M.; project administration, E.M.-S.; funding acquisition, E.M.-S. All authors have read and agreed to the published version of the manuscript.

Funding: This work was funded by the Spanish Ministerio de Ciencia e Innovación, under Project PID2020-116968RB-C31/AEI/10.13039/501100011033, by the Spanish Ministerio de Educación, Cultura y Deporte under Grant FPU16/00246, and by Spanish Ministerio de Universidades, under Programa Margarita Salas.

Conflicts of Interest: The authors declare no conflict of interest.

References

- Guo, D.; He, K.; Zhang, Y.; Song, M. A Multiband Dual-Polarized Omnidirectional Antenna for Indoor Wireless Communication Systems. *IEEE Antennas Wirel. Propag. Lett.* **2017**, *16*, 290–293. [[CrossRef](#)]
- Enomoto, J.; Nishizawa, H.; Ishikawa, R.; Takayama, Y.; Honjo, K. Parallel combination of high-efficiency amplifiers with spurious rejection for concurrent multiband operation. In Proceedings of the 2016 46th European Microwave Conference (EuMC), London, UK, 4–6 October 2016; pp. 1075–1078. [[CrossRef](#)]
- Zhang, S.; Qiu, L.; Chu, Q. Multiband Balanced Filters with Controllable Bandwidths Based on Slotline Coupling Feed. *IEEE Microw. Wirel. Components Lett.* **2017**, *27*, 974–976. [[CrossRef](#)]

4. Girbau, D.; Lazaro, A.; Perez, A.; Martinez, E.; Pradell, L.; Villarino, R. Tunable dual-band filters based on capacitive-loaded stepped-impedance resonators. In Proceedings of the 2009 European Microwave Conference (EuMC), Paris, France, 1–3 October 2019; pp. 113–116. [\[CrossRef\]](#)
5. Xu, F.; Liu, X.; Guo, H.; Wang, Y.; Mao, L. A compact dual-mode BPF base on interdigital structure. In Proceedings of the 2010 International Conference on Microwave and Millimeter Wave Technology, Chengdu, China, 8–11 May 2010; pp. 1595–1597. [\[CrossRef\]](#)
6. Ketkuntod, P.; Chomtung, P.; Meesomklin, S.; Akkaraekthalin, P. A multiband bandpass filter using interdigital and step-impedance techniques for 4G, WiMAX and WLAN systems. In Proceedings of the 2015 12th International Conference on Electrical Engineering/Electronics, Computer, Telecommunications and Information Technology (ECTI-CON), Hua Hin, Thailand, 24–26 June 2015; pp. 1–4. [\[CrossRef\]](#)
7. Psychogiou, D.; Gómez-García, R.; Peroulis, D. Single and Multiband Acoustic-Wave-Lumped-Element-Resonator (AWLR) Bandpass Filters with Reconfigurable Transfer Function. *IEEE Trans. Microw. Theory Tech.* **2016**, *64*, 4394–4404. [\[CrossRef\]](#)
8. Gómez-García, R.; Muñoz-Ferreras, J.; Psychogiou, D. Split-Type Input-Reflectionless Multiband Filters. *IEEE Microw. Wirel. Components Lett.* **2018**, *28*, 981–983. [\[CrossRef\]](#)
9. Sánchez-Martínez, J.J.; Márquez-Segura, E. Analytical Design of Wire-Bonded Multiconductor Transmission-Line-Based Ultra-Wideband Differential Bandpass Filters. *IEEE Trans. Microw. Theory Tech.* **2014**, *62*, 2308–2315. [\[CrossRef\]](#)
10. Sánchez-Martínez, J.J.; Pérez-Escribano, M.; Márquez-Segura, E. Synthesis of Dual-Band Bandpass Filters with Short-Circuited Multiconductor Transmission Lines and Shunt Open Stubs. *IEEE Access* **2019**, *7*, 24071–24081. [\[CrossRef\]](#)
11. Cameron, R.J. General coupling matrix synthesis methods for Chebyshev filtering functions. *IEEE Trans. Microw. Theory Tech.* **1999**, *47*, 433–442. [\[CrossRef\]](#)
12. Crnojević-Bengin, V. *Advances in Multi-Band Microstrip Filters*; EuMA High Frequency Technologies Series; Cambridge University Press: Cambridge, UK, 2015. [\[CrossRef\]](#)
13. Sánchez-Martínez, J.J.; Márquez-Segura, E. Analysis of wire-bonded multiconductor transmission line-based phase-shifting sections. *J. Electromagn. Waves Appl.* **2013**, *27*, 1997–2009.
14. Ou, W. Design Equations for an Interdigitated Directional Coupler. *IEEE Trans. Microw. Theory Tech.* **1975**, *23*, 253–255. [\[CrossRef\]](#)
15. Bates, R.N. Design of microstrip spur-line band-stop filters. *IEE J. Microwaves Opt. Acoust.* **1977**, *1*, 209–214. [\[CrossRef\]](#)
16. Sánchez-Martínez, J.J.; Márquez-Segura, E.; Camacho-Peñalosa, C. Analysis of Wire-Bonded Multiconductor Transmission-Line-Based Stubs. *IEEE Trans. Microw. Theory Tech.* **2013**, *61*, 1467–1476. [\[CrossRef\]](#)
17. Kirschning, M.; Jansen, R.H.; Koster, N.H.L. Accurate model for open end effect of microstrip lines. *Electron. Lett.* **1981**, *17*, 123–125. [\[CrossRef\]](#)
18. Marquez-Segura, E.; Casares-Miranda, F.; Otero, P.; Camacho-Penalosa, C.; Page, J. Analytical model of the wire-bonded interdigital capacitor. *IEEE Trans. Microw. Theory Tech.* **2006**, *54*, 748–754. [\[CrossRef\]](#)
19. Zhang, R.; Peroulis, D. Planar Multifrequency Wideband Bandpass Filters with Constant and Frequency Mappings. *IEEE Trans. Microw. Theory Tech.* **2018**, *66*, 935–942. [\[CrossRef\]](#)
20. Wu, Y.; Ma, K.; Wang, Y. Coupling Matrix Design of Compact Multiband Cascaded Trisection Bandpass Filters. *IEEE Trans. Circuits Syst. II Express Briefs* **2022**, *69*, 2762–2766. [\[CrossRef\]](#)
21. Zhao, K.; Psychogiou, D. Single-to-Multi-Band Reconfigurable Acoustic-Wave-Lumped-Resonator Bandpass Filters. *IEEE Trans. Circuits Syst. II Express Briefs* **2022**, *69*, 2066–2070. [\[CrossRef\]](#)

Disclaimer/Publisher’s Note: The statements, opinions and data contained in all publications are solely those of the individual author(s) and contributor(s) and not of MDPI and/or the editor(s). MDPI and/or the editor(s) disclaim responsibility for any injury to people or property resulting from any ideas, methods, instructions or products referred to in the content.